A route to hierarchical materials based on complexes of metallosupramolecular polyelectrolytes and amphiphiles

Dirk G. Kurth†, Pit Lehmann, and Markus Schütte

Max-Planck-Institute of Colloids and Interfaces, D-14424 Potsdam, Germany

Edited by Kenneth N. Raymond, University of California, Berkeley, CA, and approved March 9, 2000 (received for review November 5, 1999)

Anisotropic thin film materials of metallosupramolecular polyelectrolyte–amphiphile complexes (denoted PACs) with structures at several length scales were fabricated through a multistep self-assembly process. Metal ion-mediated self-assembly of the ditopic ligand 1,4-bis(2,2′:6′,2′′-terpyridine-4′-yl)benzene and electrostatic binding with the amphiphile dihexadecyl phosphate result in a PAC with tailored surface chemical properties, including solubility and surface activity. The PAC forms a stable monolayer at the air–water interface that is readily transferred and oriented on solid supports with the Langmuir–Blodgett technique. The presented strategy unifies colloid and metallosupramolecular chemistry and opens a versatile route to hierarchical materials with tailored structures and functions.

The design and construction of supramolecular architectures of nanoscopic dimensions give access to entities of increasing complexity with distinct structural and functional properties (1). The use of intermolecular forces provides a rational and efficient method to position molecular components precisely in a well defined supramolecular architecture (2). Self-assembly relies on a sequence of spontaneous recognition, growth, and termination steps to form the final equilibrium supramolecular entity (or a collection of such) through metal ion coordination, hydrogen bonds, or hydrophobic or electrostatic interactions. Applications of such systems in materials science, medicine, and chemical technology are diverse, including recognition (sensing), transformation (catalysis), and translocation (signal transduction) devices.

Although the principles that govern self-assembly of discrete supramolecular assemblies are well understood, the fabrication of (extended) structures with more than one length scale is the next challenge in the implementation of supramolecular devices in functional materials (3). Correlation of positions and orientations of the constituents in a material, preferentially over a long range, is of paramount importance to exploit the properties of supramolecular devices fully, for example in vectorial transport processes, such as light-to-energy conversion, or to establish an electronic band structure as in semiconductors (4–6). To achieve this goal, it will be necessary to improve existing and to innovate new methods to fabricate hierarchical materials. The Langmuir–Blodgett (LB) technique was one of the first methods to fabricate films with a well defined architecture and played a key role in the development of molecular electronics (7). Other approaches include the engineering of crystals (8), liquid crystalline materials, and lyotropic mesophases (9). However, the implementation of metallosupramolecular devices in ordered hierarchical architectures has not been realized to date.

Metal-ion-directed self-assembly is of particular interest for the construction of functional devices (10). Metal ions possess a range of well defined coordination geometries and diverse properties that are relevant in electronic and photonic materials (11). The particular steric and electronic ligand-metal ion interactions determine the final properties of the assembly. In principle, it is, therefore, possible to tailor the thermodynamic, kinetic, and functional properties of these devices by judicious choice of the metal ion and the ligand (12).

Metal ion directed self-assembly with ditopic terpyridine ligands results in extended, one-dimensional metallosupramolecular coordination polyelectrolytes (MEPEs; ref. 13). With oppositely charged macromolecules, MEPEs form films on various substrates, including nanoparticles, held together primarily by electrostatic interactions (14). Although this process does not require special equipment or substrates, it does not provide the degree of order demanded above (15). To fabricate well ordered materials with metallosupramolecular devices, a different approach is required. As already mentioned, highly ordered films can be fabricated by the LB method (16). The MEPEs are too hydrophilic to form pure LB films. To render the MEPE surface active for LB processing, we resorted to a colloid-chemical approach by decorating the MEPE with oppositely charged amphiphiles, a highly cooperative mechanism that results in superstructured mesophases (17).

Polyelectrolyte–Amphiphile Complex (PAC) Synthesis. As shown schematically in Fig. 1, reaction of the ditopic terpyridine ligand 1,4-bis(2,2′:6′,2′′-terpyridine-4′-yl)benzene with $Fe(OAc)_2$ results in formation of the blue colored Fe(II)-MEPE **1**. Treating an aqueous solution of **1** with a chloroform solution containing 1.5 equivalents (with respect to the charges) of DHP results in instant transfer of the Fe(II)-PAC, **2**, into the organic phase. After drying and evaporating the organic phase, **2** is isolated as dark blue powder, which is soluble in common organic solvents. Investigations by UV-visible (UV-vis), [^{1}H]NMR, and IR spectroscopy confirm the structural integrity of the Fe(II)-MEPE on complexation of the amphiphiles.‡ The [^{1}H]NMR spectra show that the acetate counter ions of **1** are replaced by amphiphiles. Quantitative examination of [^{1}H]NMR data as well as elemental analysis suggest a composition of six to seven amphiphiles perMEPE repeat unit.§ Complexation of **1** with sodium dihexyl(2-ethyl)phosphate results in a PAC of similar composition. Such nonstoichiometric compositions with respect to the number

---

This paper was submitted directly (Track II) to the PNAS office.

Abbreviation: PAC, polyelectrolyte–amphiphile complex; LB, Langmuir–Blodgett; MEPE, metallosupramolecular coordination polyelectrolyte; DHP, dihexadecyl phosphate; UV-vis, UV-visible.

†To whom reprint requests should be addressed. E-mail: dirk.kurth@mpikg-golm.mpg.de.

‡[^{1}H]NMR ($CDCl_3$): δ 0.88 (m, 6H, DHP), 1.25 (m, 52H, DHP), 1.67 (m, 4H, DHP), 4.01 (m, 4H, DHP), 7.38 (m, 4H, terpy), 7.91 (m, 4H, terpy), 8.08 (s, 4H, terpy), 8.70 (m, 4H, terpy), 8.78 (m, 4H, terpy), 8.82 (s, 4H, terpy). IR (KBr, cm^{-1}): 2,954, 2,917, 2,849, 1,467, 1,213, 1,162, 1,108, 1,081, 1,015, 929, 791, 721. UV-vis ($CDCl_3$, nm): 595, 320, 290.

§Elemental analysis calculated for $C_{228}H_{420}N_6P_6O_{24}Fe{\cdot}8\,H_2O$ (corresponding to a ratio of six surfactants per FE(II)-MEPE repeat unit): C 68.2, H 10.9, N 2.1. Found: C 68.4, H 10.6, N 2.0. Based on the accuracy of the employed methods, we estimate that six to seven surfactants bind to each MEPE repeat unit.

The publication costs of this article were defrayed in part by page charge payment. This article must therefore be hereby marked "*advertisement*" in accordance with 18 U.S.C. §1734 solely to indicate this fact.

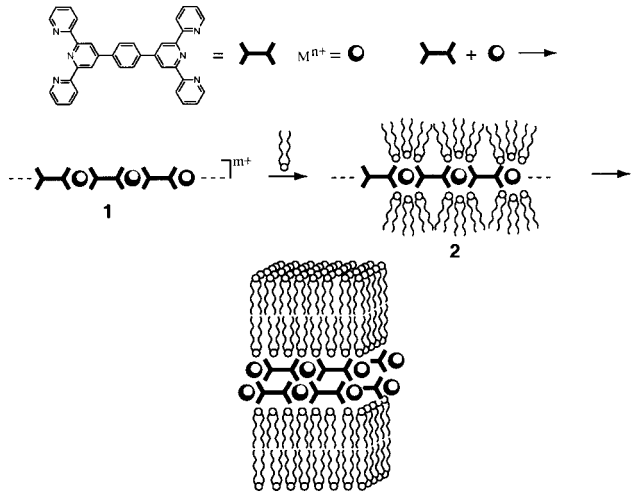

Fig. 1. Metal ion coordination of ditopic terpyridyl ligand leads to positively charged MEPEs. **1**, Subsequent reaction with the amphiphile dihexadecyl phosphate (DHP) results in the hydrophobic PAC **2**, which is soluble in common organic solvents and forms Langmuir monolayers at the air–water interface. Transfer of Langmuir monolayers onto solid substrates via the LB technique permits facile fabrication of metallosupramolecular thin films with an excellent internal order and a Y type architecture. In a facile and rational way, the architecture of the final material, including the metal–metal distances, the interlayer spacings, the orientation of each layer as well as the sequence of layers, can be controlled at every step through the used ligands, metal ions, amphiphiles, and transfer conditions.

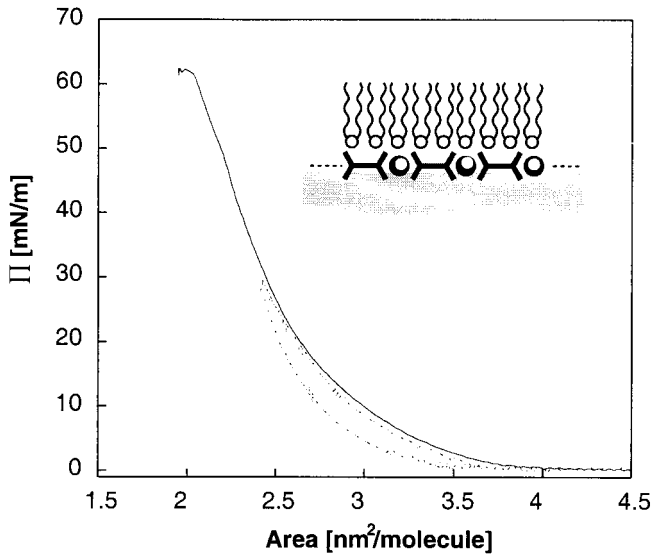

Fig. 2. Compression isotherm (solid line) and hysteresis (dotted line) of **2** at the air–water interface. The monolayer shows no distinct phase transitions. The area per molecule at the collapse pressure is ≈2.2 nm^2 per molecule corresponding to six amphiphile molecules. The collapse pressure is remarkably high. (*Inset*) Possible structure of the monolayer: the MEPE-amphiphile complex rearranges such that the amphiphiles form a top monolayer that is stabilized by electrostatic interactions with the MEPE located at the water interface.

of amphiphiles and charges are not uncommon (18). In solvents of low polarity, like chloroform, the complexes are undissociated and can be viewed as rigid cylindrical inverted micelles (19). Currently, we propose that through electrostatic and hydrophobic interactions, as well as intermolecular hydrogen bonds, the amphiphiles form aggregates primarily located around the hydrophilic parts of the Fe(II)-MEPE.

Langmuir Films. The PAC forms stable Langmuir monolayers at the air–water interface. Fig. 2 shows the surface pressure, π, versus area isotherm of **2**. The isotherm was found to be reproducible.[¶] It shows a slight hysteresis and a remarkably high collapse pressure (>60 mN/m) indicating a stable monolayer. The isotherm shows no distinct phase transitions. The area per molecule at the collapse pressure (2.2 nm^2 per molecule) corresponds to six amphiphiles. In a pure DHP Langmuir monolayer, the molecular area at the collapse pressure (48 mN/m) was determined to be 0.38 nm^2. We, therefore, propose that the PAC rearranges such that the amphiphiles form a compact monolayer located at the top, whereas the Fe(II)-MEPE is in contact with the water interface (Fig. 2 *Inset*; ref. 20). This composite structure probably enhances the stability of the Langmuir monolayer.

LB Films. Monolayers of **2** are readily transferred onto solid substrates with the LB technique.[‖] Repeated transfer leads to a multilayer film. UV-vis absorption spectra of multilayer films of **2** on quartz substrates indicate a linear film growth as well as the continuous incorporation of MEPE in the film.[**] The metal-to-ligand charge transfer band is shifted by ≈8 nm to lower energy, which is attributed to a change of polarity in the film. Linear growth of film thickness was confirmed independently by ellipsometry.[††] The average thickness per layer is 2.8 ± 0.2 nm. This value is in agreement with a monolayer. A film with the amphiphiles in an all-*trans* conformation and an upright orientation would have a thickness of 3.2 nm. Fig. 3*A* shows the ellipsometric parameters Δ in zone 1 and 3 and Ψ as a function of the azimuth defined by the dipping direction and the plane of incidence. The sinusoidal variation of these parameters indicates that the film is anisotropic. The extremities of Ψ are directly related to the directions of the optical axes. Because of symmetry considerations, the molecules are oriented either in or normal to the dipping direction. This point will be addressed below in more detail. The film structure was investigated further with x-ray reflectance. The reflectance curves for multilayers show Kiessig fringes, which indicate a homogeneous layer thickness, as well as Bragg peaks, characteristic of an internal structure (data not shown). The film thickness per layer determined by analyzing the Kiessig fringes is in agreement with the ellipsometric data. The calculated lattice spacing of 5.7 nm corresponds to a double layer. We also note that the reflectance curves of LB films made of l layers show only $l/2$ Kiessig fringes before the first-order Bragg peak. This result is an indication that the LB films are of the Y type (deposition occurs during up and down

[¶]Langmuir films of **2** were prepared with a Lauda film balance. The **2** (2.45 mg) was dissolved in 10 ml of $CHCl_3$, and 300 μl of the solution was spread onto distilled water (Milli-Q water with a resistance higher than 18.2 MΩ cm) at 20°C.

[‖]LB transfer was carried out with a Nima film balance. Quartz (Hellma Optik, Forest Hills, NY) and silicon (Wacker AG, Munich) wafers were used as substrates. The slides were deposited in the subphase before spreading. Transfer was done at a constant surface pressure of 40 mN/m and a dipping speed of 6 mm/min (temperature 20°C). The transfer ratio was always 0.95 ± 0.05 for both directions.

[**]UV-vis absorption spectra were recorded with a Varian Cary 50.

[††]Ellipsometric measurements were performed with null ellipsometry by using a Multiskop (Optrel, Berlin, Germany; 2-mW HeNe Laser; λ = 632.8 nm; angle of incidence = 70°). Films were deposited onto silicon wafers for measurements. A film refractive index of 1.58 (± 0.01) − *i* 0.017 was used. The real part of the refractive index as well as the thickness were obtained by ellipsometry from thick LB films. The imaginary part was determined from UV-vis spectra. The thickness of these samples was independently confirmed by x-ray reflectance.

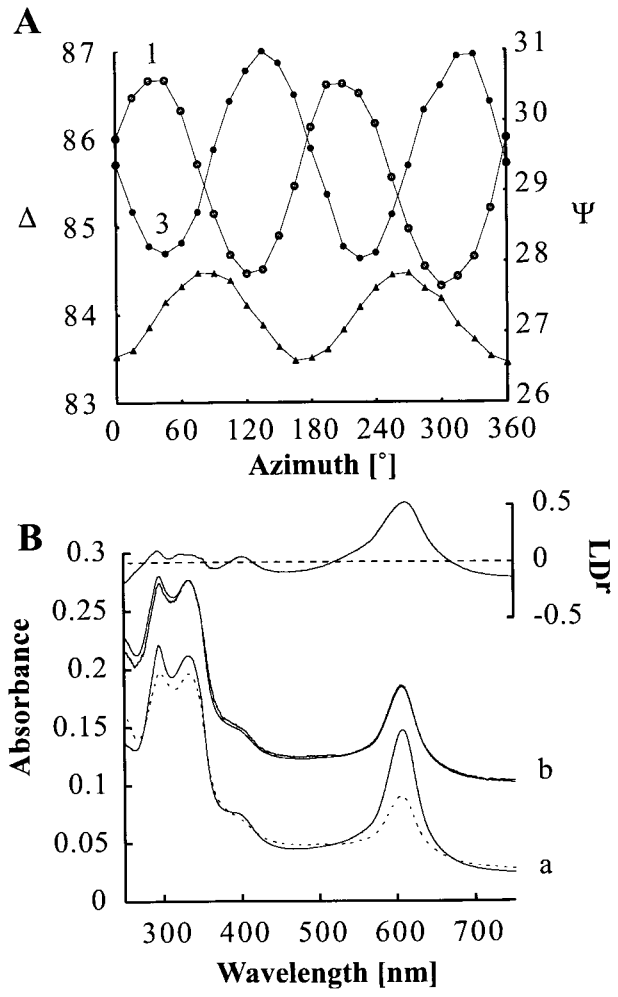

Fig. 3. (*A*) The ellipsometric parameters Δ and Ψ as a function of the azimuth defined by the dipping direction and the plane of incidence of a LB film of **2** (21 layers on silicon). The top two curves show Δ in zone 1 and 3; the bottom curve shows Ψ. The sinusoidal variation indicates that the film is anisotropic. The trace of Ψ suggests that the optical axes of the sample are either in or normal to the dipping direction. (*B*) UV-vis absorption spectra of LB-films of **2** (15 layers on both sides of the quartz substrate). (Trace a) Spectra recorded with radiation polarized parallel (solid line) and perpendicular (dotted line) to the dipping direction confirming alignment of the metallosupramolecular constituents in the LB layer. (Trace b) The traces of spectra recorded with unpolarized (3 *A*) and polarized radiation ($A_{P|_2|} + 2A_S$). The similarity of both plots suggests that the film is macroscopically uniaxial. The reduced linear dichroism (LD^r) is also shown (top spectrum). The predominantly positive LD^r of the absorption bands indicates an orientation of the PAC parallel to the dipping direction.

stroke) and consist of amphiphile/MEPE sandwich layers (see Fig. 1). This type of architecture supports the proposed structure of the Langmuir monolayer (*vide supra*). Vibrational spectroscopy reveals that the amphiphile alkyl chains are in an all-*trans* conformation with a high degree of order; the methylene C-H stretching modes occur at 2,917 and 2,849 cm^{-1} (21).

UV-Vis Dichroism. UV-vis absorption spectroscopy with polarized radiation was used to investigate a possible orientation of the Fe(II)-PAC within the LB films.[‡‡] The solid line in Fig. 3*B* represents the spectrum recorded with parallel polarized radiation, and the dotted line represents the spectrum for perpendicular polarized radiation (with respect to the dipping direction). The observed dichroism of the metal-to-ligand charge transfer, n-π^*, and π-π^* bands clearly indicates an alignment of **2**. Assuming a single linear polarized metal-to-ligand charge transfer transition, the order parameter given by $S = (2r - 1)/(2r + 2)$, where $r = A_P/A_S$, is 0.5 (22). In fact, the degree of order is higher. The value represents only a lower limit of *S*, because the assumption of a single polarized transition is only an approximation (*vide infra*). A plot of the dichroic ratio as a function of the number of layers reveals a linear relationship, indicating that the anisotropy is transfer induced and substrate independent (data not shown). In case of a macroscopically uniaxial orientation, the absorbance for unpolarized and polarized radiation is related according to $3A = A_{P|_2|} \pm 2A_S$, where A, A_P, and A_S are the absorbances recorded with unpolarized, parallel, and perpendicular polarized radiation, respectively (22). The traces of the computed and experimental spectra are very similar (Fig. 3*B*, trace b), and we, therefore, conclude that the Fe(II)-MEPE rods are uniaxially oriented.[§§] The reduced linear dichroism $LD^r = (A_P - A_S)/A$ provides further insight into the polarized absorption spectra (Fig. 3*B*). The pronounced wavelength dependence of the LD^r indicates that the absorption bands, in particular the metal-to-ligand charge transfer band, consist of more than one (polarized) transition moment (23). A positive LD^r value indicates a transition polarized parallel to the molecular axis, and a negative value is a sign for a transition polarized perpendicular to the molecular axis. The predominantly positive LD^rs lead to the conclusion that the molecular axis of the PAC is orientated parallel to the dipping direction.

A concept is presented that combines colloid, metallosupramolecular, and surface chemistry: complexation of amphiphiles and MEPEs yields materials with tailored surface chemical properties, including solubility and surface activity. The resulting PAC is soluble in common organic solvents, forms Langmuir monolayers at the air–water interface, and is readily transferred onto solid substrates. The highly organized LB film represents a supramolecular material with a hierarchical architecture. (*i*) Metal ion coordination mediates the structure at the molecular level. (*ii*) At the mesoscopic length scale, the PAC is organized through electrostatic binding and hydrophobic interactions. (*iii*) At the macroscopic level, the architecture is determined by the deposition sequence of LB transfer. Finally, the modular nature of this approach should be pointed out. The structure and functionality can be controlled at each level by choosing suitably functionalized ligands, metal ions, amphiphiles, and transfer conditions. The ease of complex formation, the availability of amphiphiles, and the diversity of metal ion coordination chemistry point to a remarkable range of possible structures and functionalities. The strategy presented herein opens a facile entry to a versatile class of building blocks to implement metallosupramolecular devices for applications that require vectorial properties, like light-harvesting devices, or positional correlation, such as ion dot information storage devices as suggested by Lehn and coworkers (24).

We thank Helmuth Möhwald for fruitful discussions and Christa Stolle for her help in the preparation of the compounds. This work was supported by the Max-Planck-Society.

[‡‡]UV-vis absorption measurements with polarized light were performed with a Varian Cary 4E. A Glan-Laser polarizer (Halle, Berlin) was used. The polarizer was kept in a fixed position while the sample was rotated.

[§§]Polarized microscopy showed uniform films with no evidence of domains (at that resolution).

1. Lehn, J.-M. (1990) *Angew. Chem. Int. Ed. Engl.* **102,** 1304–1319.
2. Whitesides, G. M., Mathias, J. P. & Seto, J. T. (1991) *Science* **254,** 1312–1319.
3. Lakes, R. (1993) *Nature (London)* **361,** 511–515.
4. Simon, J., André, J. J. & Skoulios, A. (1986) *New J. Chem.* **10,** 295–311.

5. Simon, J., Tournilhac, F. & André, J. J. (1987) *New J. Chem.* **11,** 383–399.
6. Simon, J., Bassoul, P. & Norvez, S. (1989) *New J. Chem.* **13,** 13–31.
7. Kuhn, H. & Möbius, D. (1993) in *Physical Methods of Chemistry Series*, eds. Rossiter, B. W.& Baetzold, R. C. (Wiley, New York), Vol. IX, pp. 375–542.
8. Desiraju, G. R. (1995) *Angew. Chem. Int. Ed. Engl.* **34,** 2328–2361.
9. Ober, C. K. & Wegner, G. (1997) *Adv. Mater.* **9,** 17–31.
10. Constable, E. C. (1998) *Electronic Materials: The Oligomer Approach* (VCH, New York).
11. Balzani, V. & Scandola, F. (1991) *Supramolecular Photochemistry* (Harwood, New York).
12. Lehn, J.-M. (1995) in *Supramolecular Chemistry: Concepts and Perspectives* (VCH, New York), pp. 139–195.
13. Schütte, M., Kurth, D. G., Linford, M. R., Cölfen, H. & Möhwald, H. (1998) *Angew. Chem. Int. Ed. Engl.* **37,** 2891–2893.
14. Kurth, D. G., Caruso, F. & Schüler, C. (1999) *Chem. Commun.* 1579–1580.
15. Decher, G. (1997) *Science* **277,** 1232–1237.
16. Gupta, V. K., Kornfield, J. A., Ferencz, A. & Wegner, G. (1994) *Science* **265,** 940–942.
17. Antonietti, M. & Göltner, C. (1997) *Angew. Chem. Int. Ed. Engl.* **36,** 910–928.
18. Antonietti, M., Kaul, A. & Thünemann, A. (1995) *Langmuir* **11,** 2633–2638.
19. MacKnight, W. J., Ponomarenko, E. A. & Tirrell, D. A. (1998) *Acc. Chem. Res.* **31,** 781–788.
20. Goddard, E. D. (1986) *Colloids Surf.* **19,** 301–329.
21. Snyder, R. G., Hsu, S. L. & Krimm, S. (1978) *Spectrochim. Acta* **34,** 395–406.
22. Rodger, A. & Norden, B. (1997) in *Circular Dichroism and Linear Dichroism* (University Press, Oxford), pp. 1–65.
23. Agnew, S. F., Stone, M. I. & Crosby, G. A. (1982) *Chem. Phys. Lett.* **85,** 57–60.
24. Garcia, A. M., Romero-Salguero, F. J., Bassani, D. M., Lehn, J.-M., Baum, G. & Fenske, D. (1999) *Chem. Eur. J.* **5,** 1803–1808.